Journal of Engineering and Sustainable Development
Vol. 23, No.02, March 2019
ISSN 2520-0917
https://doi.org/10.31272/jeasd.23.2.9

# MODELING AND ANALYSIS OF A FOUR-LEG INVERTER USING SPACE VECTOR PULSE WIDTH MODULATION TECHNIQUE

Dr. Isam Mahmood Abdulbaqi[1], Dr. Ali Husain Ahmed [2], Dr. Riyadh Ghanim Omar [3]
*Abdullah Sahib Abdulsada[4]

1) Prof. Electrical Engineering Department, University of Mustansiriyah, Baghdad, Iraq
2) Assistant Prof., Electrical and Electronic Engineering Department UOT, Baghdad, Iraq
3) Lecturer Electrical Engineering Department Universityof Mustansiriyah, Baghdad, Iraq
4) Ph.D. Student, Electrical and Electronic Engineering Department UOT, Baghdad, Iraq

**Abstract:** The bad effect of zero sequence current in unbalanced load when connected to three-leg inverter, is the main challenge leading to add fourth leg and using three dimensional space vector pulse width modulation (3-D) SVPWM technique to handle this problem. The paper presents an analysis and study of this technique, depending on the average large signal model. This technique simulated by using Matlab/Simulink and the results shows good performance with low THD for different operating conditions.

**Keywords:** Three-dimensional space vector modulation (3-D SVM), three-phase four-leg voltage source inverter (3P4L-VSI), Inverter-based distributed generation (IBDG), Zero Switching Vectors (ZSV), Non- Zero Switching Vector (NZSV).

## النمذجة وتحليل لمبدل رباعي الأرجل ذو تعديل عرض النبضة بأستخدام الموجه الفضائي

**الخلاصة:** التأثير السيئ لتيار التتابع الصفري عند تغذية أحمال غير متوازنة من عاكس ثلاثي الأرجل يعتبر السبب الرئيسي لأضافة الذراع الرابع واعتماد تقنية المتجه الفضائي لتضمين عرض النبضة ثلاثي الأبعاد (3-D SVPWM) لمعالجة هذه المشكلة. تقدم هذه الورقة العلمية دراسة تحليلية لهذه التقنية بأعتماد نموذج معدل الأشارة الكبيرة. تمت نمذجة هذه التقنية باستخدام برمجيات (ماتلاب-سميولنك). لقد أظهرت النتائج أداء جيد للعاكس وبمستوى تشوه كلي للتوافقيات (THD) مقبول في ظروف تشغيل مختلفة.

## 1. Introduction

In the last decades and due to the development in the power electronics sector and the increase of renewable energy utilization to produce electricity, the challenge is to design and improve an inverter-based distributed generation (IBDG) unit. Such a unit is able to produce high quality AC output three-phase voltages for a stand-alone or a grid tied systems [1].

**Corresponding Author* abdullah780s@yahoo.com

The need of three-phase four-Leg voltage source inverter (3P4L-VSI) arises to handle the neutral current in a non-linear and unbalanced load. The ultimate goal of the four-leg inverter is to have a stable three-phase output voltage with a low harmonic content under different operating conditions.

Several studies about modeling and control of 3P4L-VSI are presented in industrial application and distributed generation such as the usage of 3P4L-VSI as uninterruptible power supply in reference [2], or as a stand-alone system in reference [3]. The recent studies focused on the practical use of 3P4L-VSI as a power quality improvement as an active power filter [4].

This paper characterized by the previous work dealt with the subject; it is providing a study of multiple cases of pure resistive load, enhanced by mathematical calculations that compared with the waveforms of output voltages, line currents and neutral current.

## 2. Technical Approach to Supply Unbalanced Load

For any inverter fed star-connected 3-phase system, the neutral point problem arises when unbalanced and non-linear loads connected to such system. To maintain neutral point voltage equal to zero and to keep the supplied three phase voltages constant at a desired level for the limited extent of unbalanced load, there are many techniques adopted to deal with this problem by feeding it through [5]:

a) A delta/star (Δ/Y) transformer,
b) A split DC link capacitor with three-phase three-leg inverter,
c) A three-phase four-leg inverter using SVPWM technique shown in Fig. (1)

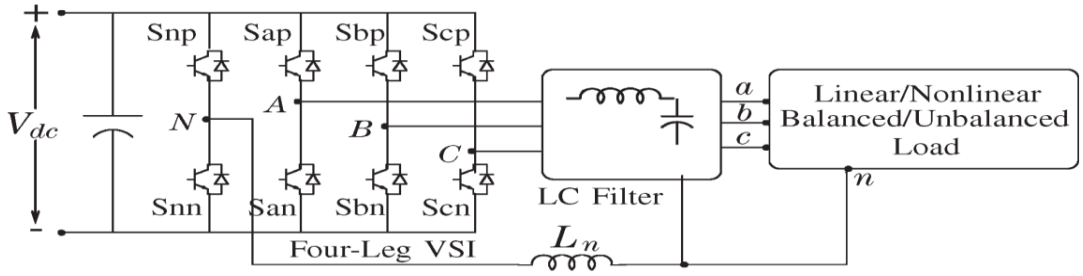


Fig. (1) Four-leg inverter configuration.

The delta/star transformer is often avoided due to cost, weight and efficiency considerations. For the split DC link capacitor approach, the three-phase converter essentially becomes three single-phase half-bridge converters, thus it suffers from an insufficient utilization of the dc link voltage. In addition, large and expensive DC link capacitors are needed to maintain an acceptable voltage ripple level across the dc link capacitors in case of a large neutral current due to unbalanced and/or nonlinear load [6]. Hence, the most preferred solution is the (4L-VSI).

## 3. Large-signal Average Model of Four-Leg Inverter

The large-signal average model of the four leg voltage source inverter (4L-VSI) is used to find a trajectory of reference voltage vector in 3-D SVM when operated in steady state condition and

design of the control loop. The large-signal average model is obtained by replacing the four-leg inverter switching network in figure (1) by average model. The AC output voltages $V_{an}$ , $V_{bn}$ and $V_{cn}$ are pulsating with sample period ($T_s$).

By applying pulse width modulation control, different values of output voltages according to the mathematical formula (1) of the moving average operand [6-7] can be obtained.

$$X_t = \frac{1}{T_s} \int_{t-T_s}^{t} X_\tau \, d_\tau \qquad (1)$$

Then the average AC output voltage of three phases $V_{an}$ , $V_{bn}$ , $V_{cn}$ and $I_{dc} = I_p$ are expressed as:

$$[V_{an}\ V_{bn}\ V_{cn}]^T = E \cdot [d_{an}\ d_{bn} d_{cn}]^T \qquad (2)$$

$$I_p = [d_{an}\ d_{bn}\ d_{cn}] \cdot [I_a\ \ I_b\ \ I_c]^T \qquad (3)$$

where $d_{an}, d_{bn}$ and $d_{cn}$ are line-to-neutral duty ratios based on (2) and (3), the average large-signal circuit model of the four-legged switching network is shown in Fig. (2) [8].

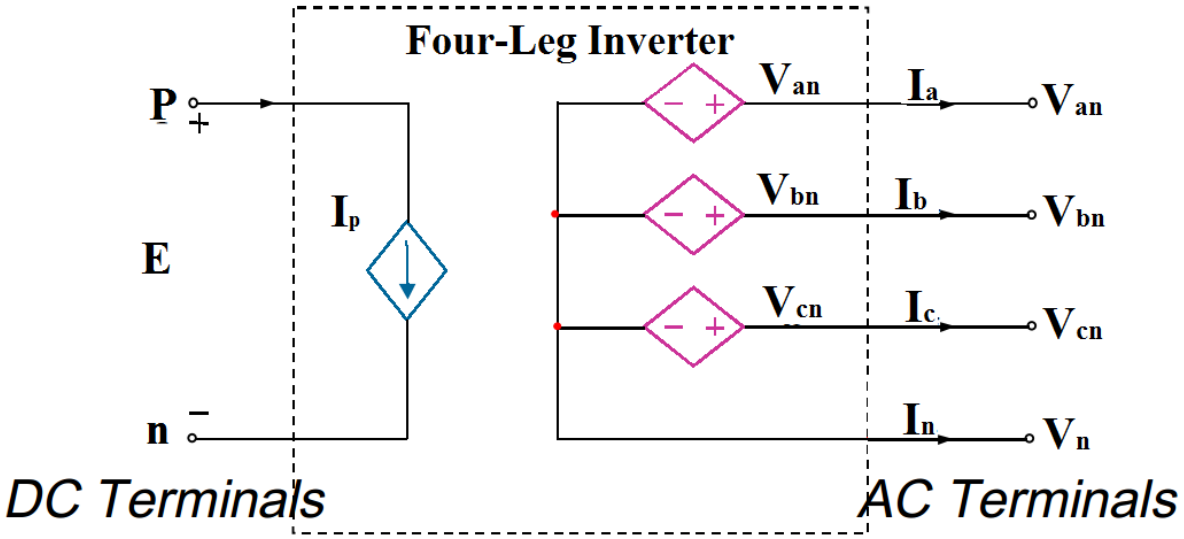


Fig. (2) average large-signal model of the four-legged switching network.

Replacing the four-leg switching network shown in Fig. (1) with the averaged switching network model, the large-signal average circuit model of the four-leg inverter in the $(a, b, c)$ coordinate is shown in Fig. (3).

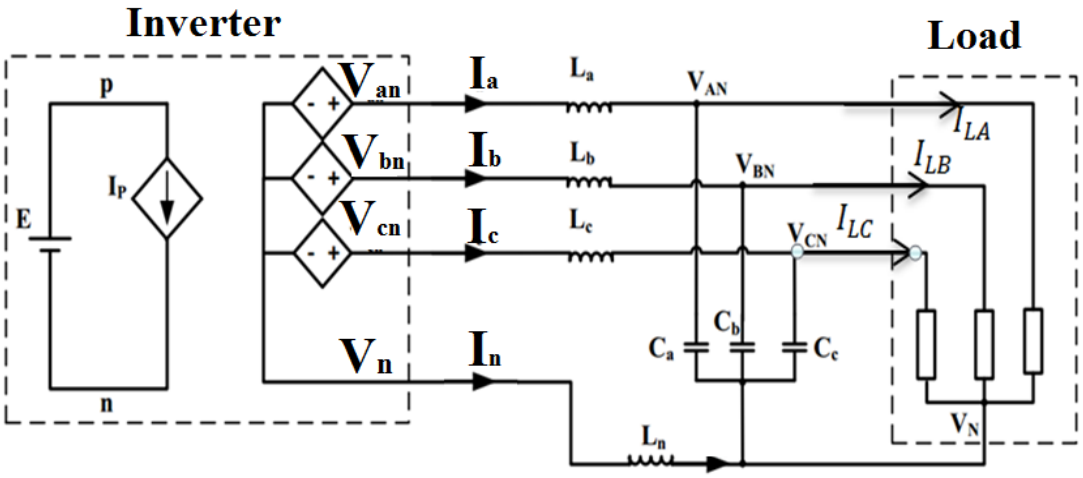


Fig. (3) Average large-signal model of four-leg inverter.

From the large-signal average circuit model of the four-leg inverter shown in Fig. (3), the following equations derived using KVL and KCL [7].

$$\begin{bmatrix} V_{an} \\ V_{bn} \\ V_{cn} \end{bmatrix} = \begin{bmatrix} L\left(\frac{di_{LA}}{dt} + C\frac{d^2 v_{AN}}{dt^2}\right) + V_{AN} - L_n\frac{di_n}{dt} \\ L\left(\frac{di_{LB}}{dt} + C\frac{d^2 v_{BN}}{dt^2}\right) + V_{BN} - L_n\frac{di_n}{dt} \\ L\left(\frac{di_{LC}}{dt} + C\frac{d^2 v_{CN}}{dt^2}\right) + V_{CN} - L_n\frac{di_n}{dt} \end{bmatrix} \quad (4)$$

$$i_n = -(i_{LA} + i_{LB} + i_{LC}) - C\frac{d(v_{AN}+v_{BN}+v_{CN})}{dt} \quad (5)$$

Where $i_{LA}, i_{LB}$ and $i_{LC}$ are load three phase currents and $i_n$ is the neutral current.

The reference control voltage in the $(a, b, c)$ coordinate $[V_{an-ref}, V_{bn-ref}, V_{cn-ref}]^T$ can be calculated from (4) and (5) for a given load [9].

## 4. Analysis of Space Vector Modulation in Four-Leg Inverter Technique.

At 1998, Richard Zhang made a new approach for three-dimensional space vector modulation (3-D-SVM) to control voltage output of four-leg voltage source inverter supplying three phase unbalance or non-linear loads [10, 11].

According to this approach after adding the fourth leg to the three-leg inverter, the switching states increase from eight states in three-leg inverter to 16 switching states in four-leg inverter [6].

This approach depends on the transformation of variables in $a, b, c$ coordinates $X_{abc}$ into an orthogonal $X_{\alpha\beta\gamma}$ coordinate in a three dimensional space.

Let $X$ represent voltage or current for three-phase four-leg inverter

$$X = X_\alpha + jX_\beta + kX_\gamma \quad (6)$$

The transformation to $V_{\alpha\beta\gamma}$ coordinate derived as below:

$$\left[V_{\alpha n-ref}\ V_{\beta n-ref} V_{\gamma n-ref}\right]^T = T.\left[V_{an-ref}\ V_{bn-ref} V_{cn-ref}\right]^T \qquad (7)$$

The operation of three-leg inverter (3LI) divided into six sectors depending on the magnitude value of $(\alpha,\ \beta)$ to determine the angle of the reference vector as explained in the equation below.

$$\text{Sector No.} = \begin{cases} 1 & \text{for} \quad 0 \le \theta < \frac{\pi}{3} \\ 2 & \text{for} \quad \frac{\pi}{3} \le \theta < \frac{2\pi}{3} \\ 3 & \text{for} \quad \frac{2\pi}{3} \le \theta < \pi \\ 4 & \text{for} \quad \pi \le \theta < \frac{4\pi}{3} \\ 5 & \text{for} \quad \frac{4\pi}{3} \le \theta < \frac{5\pi}{3} \\ 6 & \text{for} \quad \frac{5\pi}{3} \le \theta < 2\pi \end{cases} \qquad (8)$$

In three-legged inverter of an eight $(2^3 = 8)$ switching states combination, $(000,001,010,011,100,101,110,111)$ two of them $(000\ \&\ 111)$ called zero switching vectors (ZSV) and another six states non-zero switching vector (NZSV).

On the other hand, in the Four-Leg Inverter (4LI) $(2^4 = 16)$ there are sixteen switching states, which expressed in the tables (1&2) below and graphically as shown in Fig. (4).

The two switching states $0000\ \&\ 1111$ are called zero switching vectors ZSV's located at the origin point of the $(\alpha, \beta, \gamma)$ coordinate and the other fourteen active none zero switching vectors are located in different six layers depend on the level of $\gamma$ as shown Fig. (4) .

Table (1) Equivalent voltage in $(a, b, c)$corresponding to switching state

| | **0000** | **0001** | **0010** | **0011** | **0100** | **0101** | **0110** | **0111** |
|---|---|---|---|---|---|---|---|---|
| $V_a$ | 0 | −E | 0 | −E | 0 | −E | (-2/3)E | **0** |
| $V_b$ | 0 | −E | 0 | −E | E | 0 | 0 | **E** |
| $V_c$ | 0 | −E | E | −0 | 0 | −E | (2/3)E | **E** |

| | **1000** | **1001** | **1010** | **1011** | **1100** | **1101** | **1110** | **1111** |
|---|---|---|---|---|---|---|---|---|
| $V_a$ | E | 0 | E | 0 | E | 0 | E | **0** |
| $V_b$ | 0 | −E | 0 | −E | E | 0 | E | **0** |
| $V_c$ | 0 | −E | E | 0 | 0 | −E | E | **0** |

Table (2) Equivalent voltage in$(\alpha, \beta, \gamma)$corresponding to switching state

| | **0000** | **0001** | **0010** | **0011** | **0100** | **0101** | **0110** | **0111** |
|---|---|---|---|---|---|---|---|---|
| $V_\alpha$ | 0 | 0 | (-1/3)$E$ | (-1/3)$E$ | (-1/3)$E$ | (-1/3)$E$ | (-2/3)$E$ | (-2/3)$E$ |
| $V_\beta$ | 0 | 0 | (-1/√3)$E$ | (-1/√3)E | (1/√3)$E$ | (1/√3)$E$ | 0 | **0** |
| $V_\gamma$ | 0 | −E | (1/3)E | (-2/3)E | (1/3)E | (-2/3)E | (2/3)E | (-1/3)**E** |

| | **1000** | **1001** | **1010** | **1011** | **1100** | **1101** | **1110** | **1111** |
|---|---|---|---|---|---|---|---|---|
| $V_\alpha$ | (2/3)E | (2/3)E | (1/3)E | (1/3)E | (1/3)E | (1/3)E | 0 | **0** |
| $V_\beta$ | 0 | 0 | (-1/√3)E | (-1/√3)E | (1/√3)E | (1/√3)E | 0 | **0** |
| $V_\gamma$ | (1/3)E | -2/3 E | (2/3)E | (-1/3)E | (2/3)E | (-1/3)E | E | **0** |

When unbalanced load connected with output of four-leg inverter then

$$V_{an} \neq V_{bn} \neq V_{cn} \quad (9)$$

$$V_{an} + V_{bn} + V_{cn} \neq 0 \quad (10)$$

$$I_n = I_a + I_b + I_c \neq 0 \quad (11)$$

Apply transformation equation (7) on the load voltage results as:

$$\begin{bmatrix} V_{\alpha n-ref} \\ V_{\beta n-ref} \\ V_{\gamma n-ref} \end{bmatrix} = \frac{2}{3} \begin{bmatrix} 1 & -\frac{1}{2} & -\frac{1}{2} \\ 0 & \frac{\sqrt{3}}{2} & -\frac{\sqrt{3}}{2} \\ \frac{1}{2} & \frac{1}{2} & \frac{1}{2} \end{bmatrix} \begin{bmatrix} V_{an-ref} \\ V_{bn-ref} \\ V_{cn-ref} \end{bmatrix} \quad (12)$$

That's produce (γ) axis arise with different values in a positive and negative direction which depend on the zero sequence component of $(V\&I)$, this officiates to assign vector have three dimensions in $(\alpha, \beta, \gamma)$ coordinates, each vector has spire which graphically represented as shown in Fig. (4).

## 5. Space Vector Modulation in Four-Leg Inverter Technique. [6,9,12,13]

For the sake of achieving balanced 3-phase output voltages feeding an unbalanced load at steady state, the following steps must be implemented:

a. Selection of adequate switching vector sequence pattern.
b. The transformation of the reference vector $(V_{ref})$ from $V_{abc}$ coordinate to $V_{\alpha\beta\gamma}$ coordinate.
c. Determine of prism and tetrahedron.
d. Determine duty ratios of all four legs.

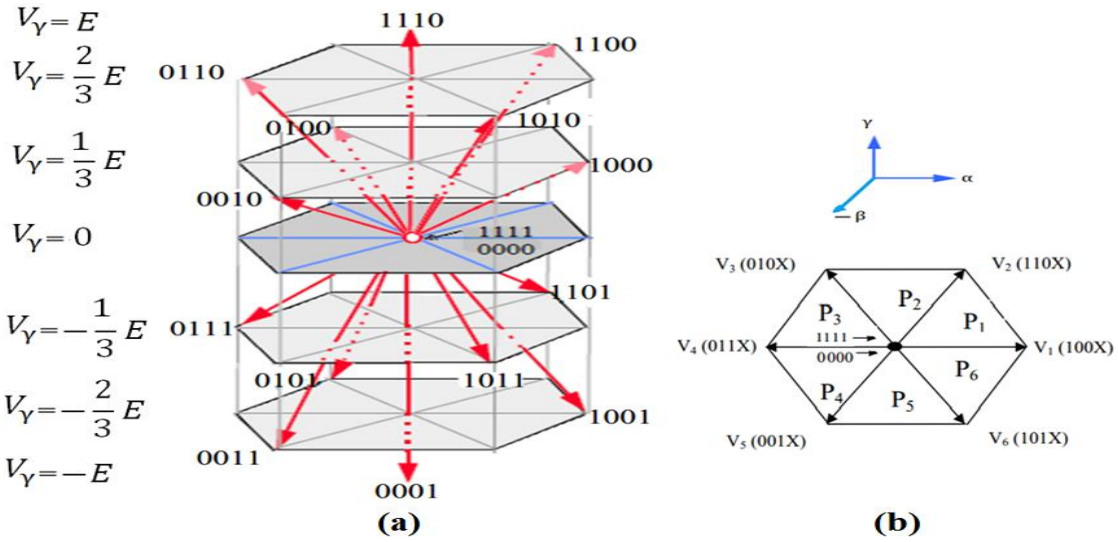


Fig. (4) (a) 4LI switching vector distribution and (b) Middle layer in SVM-4LI.

### *5.1 Sequencing of the Switching Vectors*

The sequence pattern of the 3D-SVM classified into two classes as same as 2D-SVM as follows:

Class I: This pattern uses both the two zero switching vectors 0000 & 1111.

Class II: This pattern uses only one of zero switching vectors 0000 , or 1111.

Each class has four sequencing schemes:

a. Rising edge alignment
b. Falling edge alignment
c. Symmetrical alignment
d. An alternative sequence alignment

In this study, the symmetrical alignment sequencing scheme with class I adopted as shown in Fig. (5).

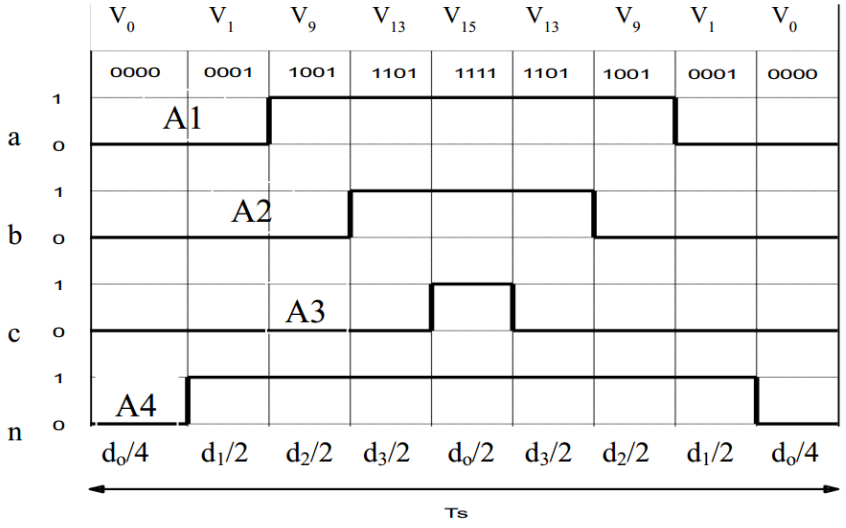


Fig. (5) Symmetrical switching sequence aligned in first tetrahedron.

### *5.2 Transformation of Output Voltages to a Stationary Reference Frame*

Transformation of reference voltages $[V_{an-ref}\ V_{bn-ref} V_{cn-ref}]^T$ into the αβγ coordinate, the reference voltage is expressed as $[V_{\alpha n-ref}\ V_{\beta n-ref} V_{\gamma n-ref}]^T$, the transformation is achieved by applying Clark's equation no. (12).

### *5.3 Projection Matrix Identification.*

#### *5.3.1 Prism Identification*

The standard method used in 3D-SVM is the same as in 2D-SVM. It depends on the value of $V_{\alpha-ref}$ and $V_{\beta-ref}$ as describe in equation No. (8) and shown in Fig. (4-b). There are six triangular prisms obtained (triangular prism 1 to triangular prism 6) as shown in Fig. (6) the angle of each triangular prism section is equal to 60 degrees, each triangular prism contains eight switching vectors, two of them is zero switching vectors 0000 & 1111 and others six non-zero switching vectors are distributed according to the value of $V_{\gamma-ref}$.

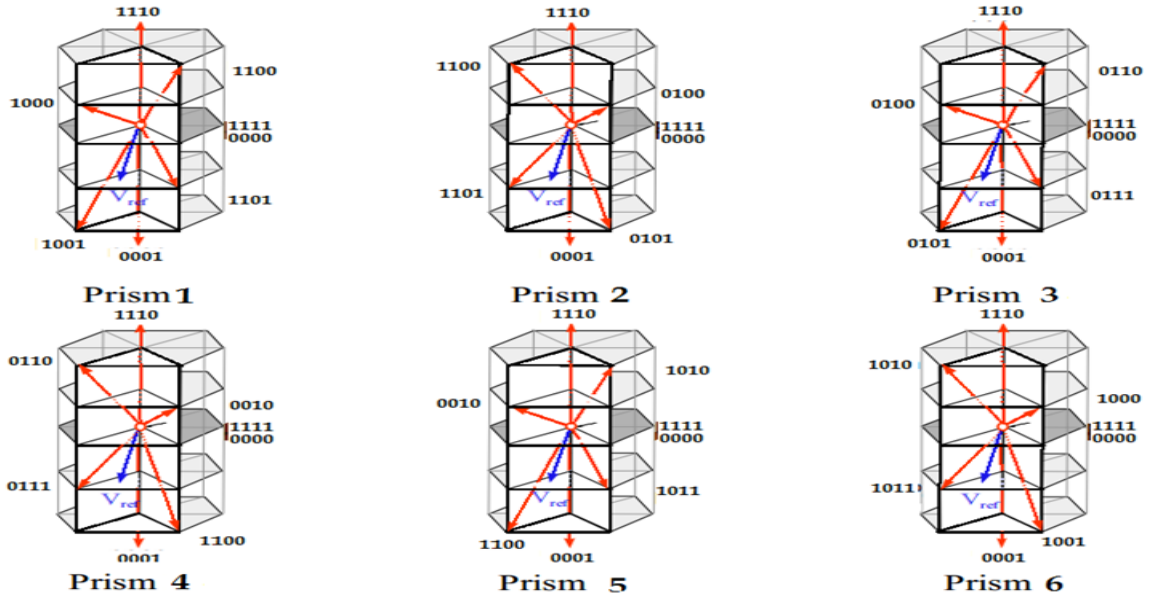


Fig. (6) Representation of six prism triangle.

#### *5.3.2 Tetrahedron Identification*

After prism identification, it is then divided into four regions with four faces called tetrahedron. Each tetrahedron contains three NZSV and two ZSV as shown in Fig. (7). The selection of adjacent switching vectors in tetrahedron occurs according to the minimum circulating energy and non-conflicting line to neutral voltage. Each tetrahedron has a particular matrix, which means there are 24 matrices as depicted in table (3 and 4) which cover all switching states for different operation condition.

*5.3.3. Duty cycle calculation*

After determining the projection of $V_{ref}$ in any tetrahedron, this means one can resolve $V_{ref}$ into three components $[V_{\alpha-ref}\ V_{\beta-ref} V_{\gamma-ref}]$. Each component represents switching vector in the same tetrahedron, for example, take prism No.1 and tetrahedron No.1 which have three NZSV(1000), (1001), (1101) and two ZSV (0000 & 1111).

The calculation of the corresponding duty ratio of each switching vector can be done after matrix determination for the tetrahedron contain $V_{ref}$ and apply equation (12).

$$V_{ref} = d_1.V_1 + d_2.V_2 + d_3.V_3 \qquad (13)$$

$$\begin{bmatrix} d_1 \\ d_2 \\ d_3 \end{bmatrix} = \frac{1}{E} \begin{bmatrix} 1 & 0 & 1 \\ \frac{1}{2} & -\frac{\sqrt{3}}{2} & -1 \\ 0 & \sqrt{3} & 0 \end{bmatrix} \begin{bmatrix} V_{\alpha n-ref} \\ V_{\beta n-ref} \\ V_{\gamma n-ref} \end{bmatrix} \qquad (14)$$

$$d_0 = 1 - d_1 - d_2 - d_3 \qquad (15)$$

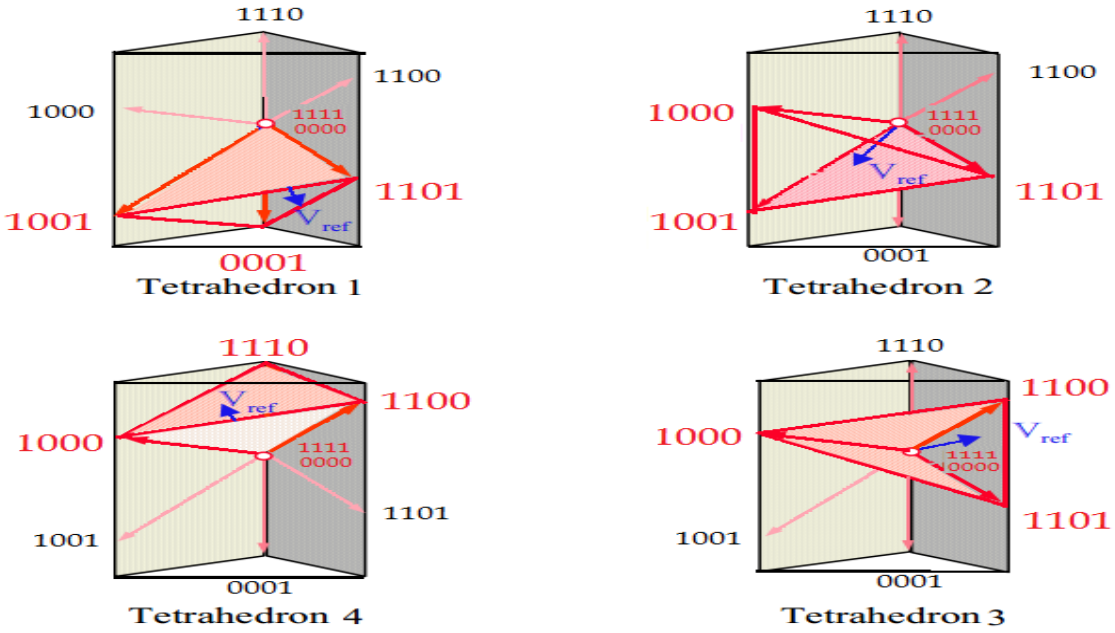


Fig. (7) Tetrahedron representation in prism No.1.

When the reference vector located in other tetrahedron, one must replace projection matrix in equation (14) for this calculation and use table (3) which shows 24 cases for non-zero switching vectors and table (4) which represents 24 projection matrices corresponding to $V_{\alpha\beta\gamma-ref}$ state.

Table (3) Non-zero switching vectors sequence V1 → V2 → V3

| Tetrahedron / Prism | 1 | 2 | 3 | 4 |
|---|---|---|---|---|
| 1 | $V1 = 1000$<br>$V2 = 1001$<br>$V3 = 1101$ | $V1 = 1000$<br>$V2 = 1100$<br>$V3 = 1101$ | $V1 = 1000$<br>$V2 = 1100$<br>$V3 = 1110$ | $\boldsymbol{V1 = 0001}$<br>$\boldsymbol{V2 = 1001}$<br>$\boldsymbol{V3 = 1101}$ |
| 2 | $V1 = 0100$<br>$V2 = 0101$<br>$V3 = 1101$ | $V1 = 0100$<br>$V2 = 1100$<br>$V3 = 1101$ | $V1 = 0100$<br>$V2 = 1100$<br>$V3 = 1110$ | $\boldsymbol{V1 = 0001}$<br>$\boldsymbol{V2 = 0101}$<br>$\boldsymbol{V3 = 1101}$ |
| 3 | $V1 = 0100$<br>$V2 = 0101$<br>$V3 = 0111$ | $V1 = 0100$<br>$V2 = 0110$<br>$V3 = 0111$ | $V1 = 0100$<br>$V2 = 0110$<br>$V3 = 0111$ | $\boldsymbol{V1 = 0001}$<br>$\boldsymbol{V2 = 0101}$<br>$\boldsymbol{V3 = 0111}$ |
| 4 | $V1 = 0010$<br>$V2 = 0011$<br>$V3 = 0111$ | $V1 = 0010$<br>$V2 = 0110$<br>$V3 = 0111$ | $V1 = 0010$<br>$V2 = 0110$<br>$V3 = 1110$ | $\boldsymbol{V1 = 0001}$<br>$\boldsymbol{V2 = 0011}$<br>$\boldsymbol{V3 = 0111}$ |
| 5 | $V1 = 0010$<br>$V2 = 0011$<br>$V3 = 1011$ | $V1 = 0010$<br>$V2 = 1010$<br>$V3 = 1011$ | $V1 = 0010$<br>$V2 = 1010$<br>$V3 = 1110$ | $\boldsymbol{V1 = 0001}$<br>$\boldsymbol{V2 = 0011}$<br>$\boldsymbol{V3 = 1011}$ |
| 6 | $V1 = 1000$<br>$V2 = 1001$<br>$V3 = 1011$ | $V1 = 1000$<br>$V2 = 1010$<br>$V3 = 1011$ | $V1 = 1000$<br>$V2 = 1010$<br>$V3 = 1110$ | $\boldsymbol{V1 = 0001}$<br>$\boldsymbol{V2 = 1001}$<br>$\boldsymbol{V3 = 1011}$ |

Table (4) Matrices projection

| Tetrahedron / Prism | 1 | 2 | 3 | 4 |
|---|---|---|---|---|
| 1 | $\begin{bmatrix} 1 & 0 & 1 \\ \frac{1}{2} & -\frac{\sqrt{3}}{2} & -1 \\ 0 & \sqrt{3} & 0 \end{bmatrix}$ | $\begin{bmatrix} \frac{3}{2} & -\frac{\sqrt{3}}{2} & 0 \\ -\frac{1}{2} & \frac{\sqrt{3}}{2} & 1 \\ \frac{1}{2} & \frac{\sqrt{3}}{2} & -1 \end{bmatrix}$ | $\begin{bmatrix} \frac{3}{2} & -\frac{\sqrt{3}}{2} & 0 \\ 0 & \sqrt{3} & 0 \\ -\frac{1}{2} & -\frac{\sqrt{3}}{2} & 1 \end{bmatrix}$ | $\begin{bmatrix} \boldsymbol{-1} & \boldsymbol{0} & \boldsymbol{-1} \\ \boldsymbol{\frac{3}{2}} & \boldsymbol{-\frac{\sqrt{3}}{2}} & \boldsymbol{0} \\ \boldsymbol{0} & \boldsymbol{\sqrt{3}} & \boldsymbol{0} \end{bmatrix}$ |
| 2 | $\begin{bmatrix} -\frac{1}{2} & \frac{\sqrt{3}}{2} & 1 \\ -1 & 0 & -1 \\ \frac{3}{2} & \frac{\sqrt{3}}{2} & 0 \end{bmatrix}$ | $\begin{bmatrix} -\frac{3}{2} & \frac{\sqrt{3}}{2} & 0 \\ 1 & 0 & 1 \\ \frac{1}{2} & \frac{\sqrt{3}}{2} & -1 \end{bmatrix}$ | $\begin{bmatrix} -\frac{3}{2} & \frac{\sqrt{3}}{2} & 0 \\ \frac{3}{2} & \frac{\sqrt{3}}{2} & 0 \\ -\frac{1}{2} & -\frac{\sqrt{3}}{2} & 1 \end{bmatrix}$ | $\begin{bmatrix} \boldsymbol{\frac{1}{2}} & \boldsymbol{-\frac{\sqrt{3}}{2}} & \boldsymbol{-1} \\ \boldsymbol{-\frac{3}{2}} & \boldsymbol{\frac{\sqrt{3}}{2}} & \boldsymbol{0} \\ \boldsymbol{\frac{3}{2}} & \boldsymbol{\frac{\sqrt{3}}{2}} & \boldsymbol{0} \end{bmatrix}$ |
| 3 | $\begin{bmatrix} -\frac{1}{2} & \frac{\sqrt{3}}{2} & 1 \\ \frac{1}{2} & \frac{\sqrt{3}}{2} & -1 \\ -\frac{3}{2} & -\frac{\sqrt{3}}{2} & 0 \end{bmatrix}$ | $\begin{bmatrix} 0 & \sqrt{3} & 0 \\ -\frac{1}{2} & -\frac{\sqrt{3}}{2} & 1 \\ -1 & 0 & -1 \end{bmatrix}$ | $\begin{bmatrix} 0 & \sqrt{3} & 0 \\ -\frac{3}{2} & -\frac{\sqrt{3}}{2} & 0 \\ 1 & 0 & 1 \end{bmatrix}$ | $\begin{bmatrix} \boldsymbol{\frac{1}{2}} & \boldsymbol{-\frac{\sqrt{3}}{2}} & \boldsymbol{-1} \\ \boldsymbol{0} & \boldsymbol{\sqrt{3}} & \boldsymbol{0} \\ \boldsymbol{-\frac{3}{2}} & \boldsymbol{-\frac{\sqrt{3}}{2}} & \boldsymbol{0} \end{bmatrix}$ |

| | | | | |
|---|---|---|---|---|
| 4 | $\begin{bmatrix} -\frac{1}{2} & -\frac{\sqrt{3}}{2} & 1 \\ \frac{1}{2} & -\frac{\sqrt{3}}{2} & -1 \\ -\frac{3}{2} & \frac{\sqrt{3}}{2} & 0 \end{bmatrix}$ | $\begin{bmatrix} 0 & -\sqrt{3} & 0 \\ -\frac{1}{2} & \frac{\sqrt{3}}{2} & 1 \\ -1 & 0 & -1 \end{bmatrix}$ | $\begin{bmatrix} 0 & -\sqrt{3} & 0 \\ -\frac{3}{2} & \frac{\sqrt{3}}{2} & 0 \\ 1 & 0 & 1 \end{bmatrix}$ | $\begin{bmatrix} \mathbf{\frac{1}{2}} & \mathbf{\frac{\sqrt{3}}{2}} & \mathbf{-1} \\ \mathbf{0} & \mathbf{-\sqrt{3}} & \mathbf{0} \\ \mathbf{-\frac{3}{2}} & \mathbf{\frac{\sqrt{3}}{2}} & \mathbf{0} \end{bmatrix}$ |
| 5 | $\begin{bmatrix} -\frac{1}{2} & -\frac{\sqrt{3}}{2} & 1 \\ -1 & 0 & -1 \\ \frac{3}{2} & -\frac{\sqrt{3}}{2} & 0 \end{bmatrix}$ | $\begin{bmatrix} -\frac{3}{2} & -\frac{\sqrt{3}}{2} & 0 \\ 1 & 0 & 1 \\ \frac{1}{2} & -\frac{\sqrt{3}}{2} & -1 \end{bmatrix}$ | $\begin{bmatrix} -\frac{3}{2} & -\frac{\sqrt{3}}{2} & 0 \\ \frac{3}{2} & -\frac{\sqrt{3}}{2} & 0 \\ -\frac{1}{2} & \frac{\sqrt{3}}{2} & 1 \end{bmatrix}$ | $\begin{bmatrix} \mathbf{\frac{1}{2}} & \mathbf{\frac{\sqrt{3}}{2}} & \mathbf{-1} \\ \mathbf{-\frac{3}{2}} & \mathbf{-\frac{\sqrt{3}}{2}} & \mathbf{0} \\ \mathbf{\frac{3}{2}} & \mathbf{-\frac{\sqrt{3}}{2}} & \mathbf{0} \end{bmatrix}$ |
| 6 | $\begin{bmatrix} 1 & 0 & 1 \\ \frac{1}{2} & \frac{\sqrt{3}}{2} & -1 \\ 0 & -\sqrt{3} & 0 \end{bmatrix}$ | $\begin{bmatrix} \frac{3}{2} & \frac{\sqrt{3}}{2} & 0 \\ -\frac{1}{2} & -\frac{\sqrt{3}}{2} & 1 \\ \frac{1}{2} & -\frac{\sqrt{3}}{2} & -1 \end{bmatrix}$ | $\begin{bmatrix} \frac{3}{2} & \frac{\sqrt{3}}{2} & 0 \\ 0 & -\sqrt{3} & 0 \\ -\frac{1}{2} & \frac{\sqrt{3}}{2} & 1 \end{bmatrix}$ | $\begin{bmatrix} \mathbf{-1} & \mathbf{0} & \mathbf{-1} \\ \mathbf{\frac{3}{2}} & \mathbf{\frac{\sqrt{3}}{2}} & \mathbf{0} \\ \mathbf{0} & \mathbf{-\sqrt{3}} & \mathbf{0} \end{bmatrix}$ |

## 6. Three-phase Four-Leg Inverter Model in Matlab/Simulink Model

Matlab/Simulink software models shown in Fig. (8) represent all the required stages to produce SVPWM, the control and the power stage.

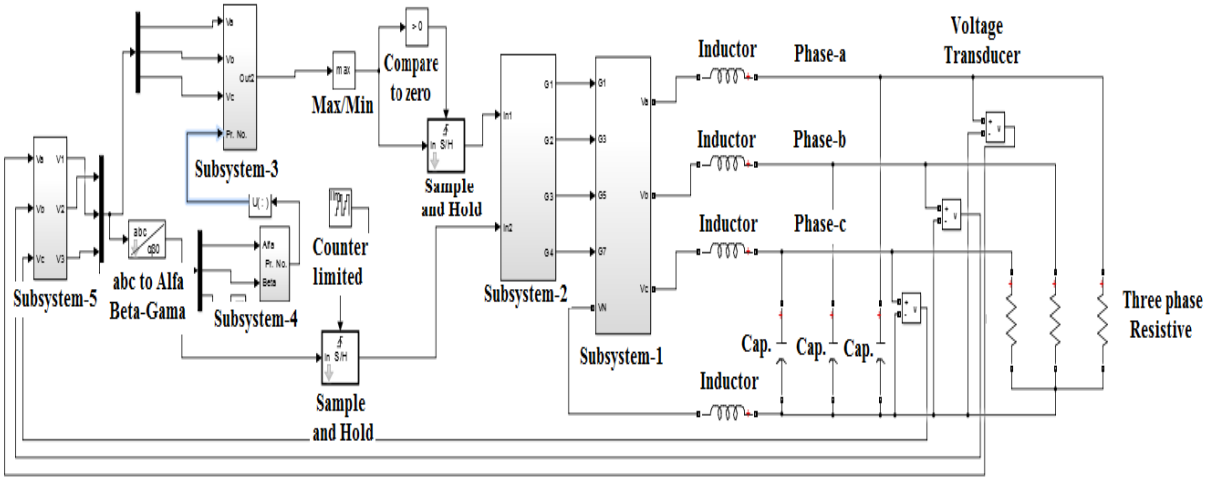


Fig. (8) Matlab/Simulink model of four-leg inverter.

Subsystem (4) that is illustrated in Fig. (9) receives the data of $V_\alpha$ and $V_\beta$ that produce after the transformation of the output voltages $V_a$, $V_b$ and $V_c$. This will lead to determining the prism number as explained in section (5.3.1).

Subsystem (3) illustrated in Fig. (10). It receives data from subsystem (3) with output voltage $V_a$, $V_b$ and $V_c$, handles these data according to paragraph (5.3.2) to determine the tetrahedrons that corresponds each prism as explained in the tables (3 and 4).

Subsystem (2) in Fig. (8) process the data from subsystem (2 and 3) that contain the sampled data $V_\alpha$, $V_\beta$, $V_\gamma$, prism No., tetrahedron number, sequence pattern, sample time ($T_s$). Then handle

this data as explained in section (5.3.3) to determine the durations $d_1, d_2, d_3$ and $d_0$ to produce pulses for upper transistor$T_1, T_3, T_5$ and $T_7$ of the inverter. On the other hand, these pulses inverted to energize the lower transistors $T_4, T_6, T_2$ and $T_8$ respectively with take dead time effect in the account, to prevent short circuit across the DC supply at any interval.

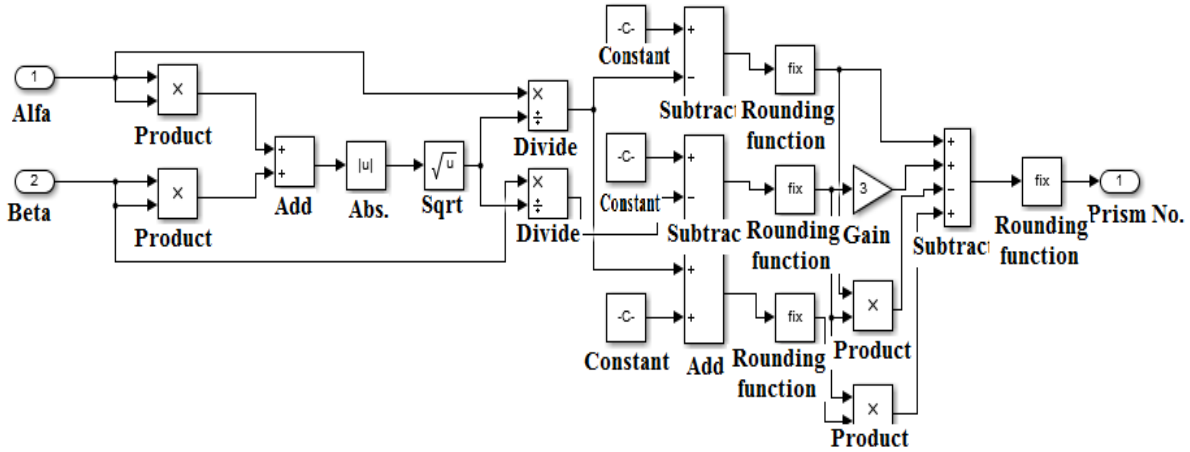


Fig. (9) Prism identification.

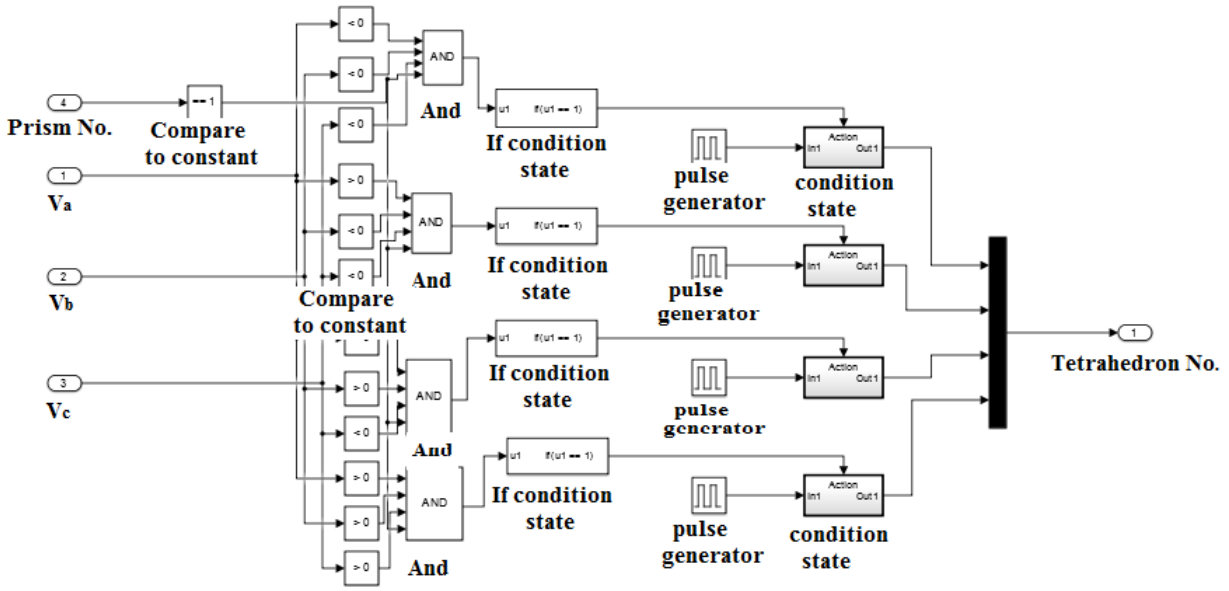


Fig. (10) Tetrahedron identification of each prism.

## 7. Simulation Results and Discussion

A Matlab/Simulink program adopted to simulate the proposed system (the four-leg inverter that uses SVPWM technique) to validate the efficient performance and to handle different loading conditions described below:

1- Balanced load
2- Unbalanced load
3- Heavy unbalanced load

These three cases have the following parameters:

1- DC link voltage = 650V
2- Filter capacitor $C = 150$ µF
3- Filter inductor $L = 1$ mH
4- Neutral inductor $L = 0.5$ mH
5- Switching frequency $Fs = 12$ kHz
6- Modulation index=0.829
7- Unbalance load resistance ($R_a = 80\Omega$ , $R_b = 100\Omega, R_c = 150\ \Omega$)

Case 1: Balanced loading

If the inverter loaded by a three-phase balanced load, a balanced currents appears in all phases ($I_a = 4.01\angle 0^\circ$ , $I_b = 4.01\angle -120^\circ, I_c = 4.01\angle -240^\circ$ ). Fig. (11) shows the waveforms of line and neutral currents and their corresponding output voltages shown in Fig. (12). Fig.s (13) illustrate the harmonic distribution spectrum of phase current (a).

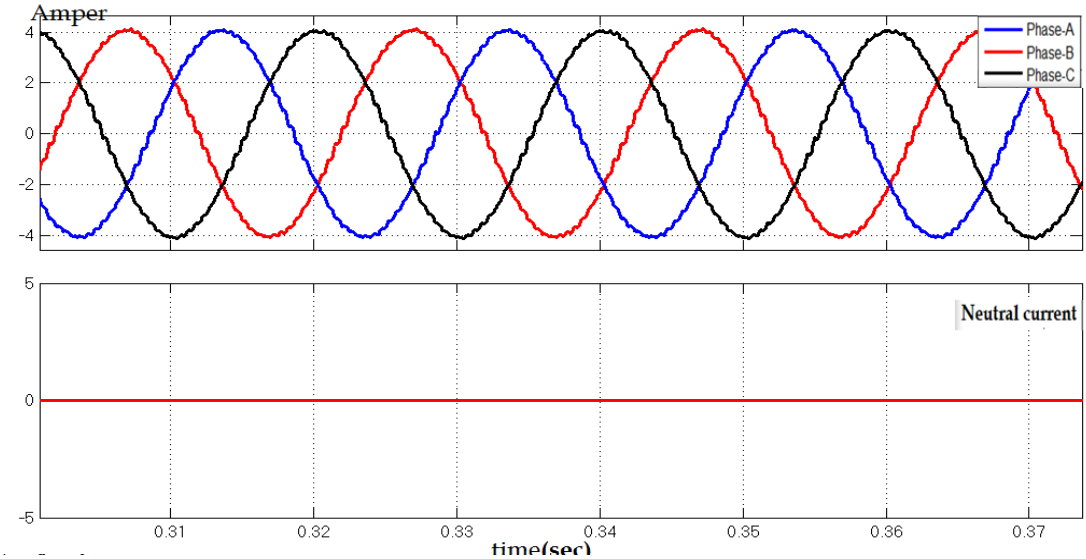


Fig. (11) waveforms of the three-phase and neutral currents.

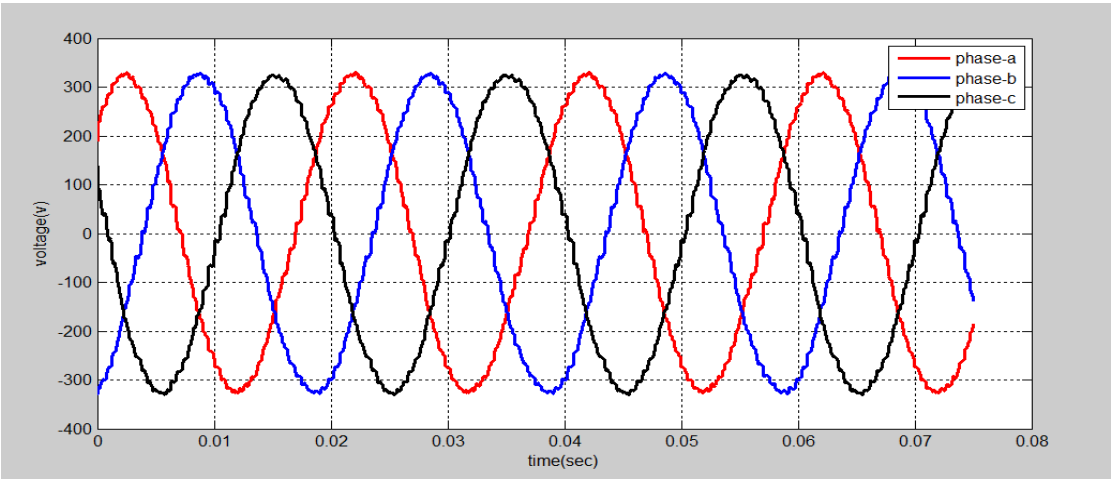


Fig. (12) output voltage waveforms.

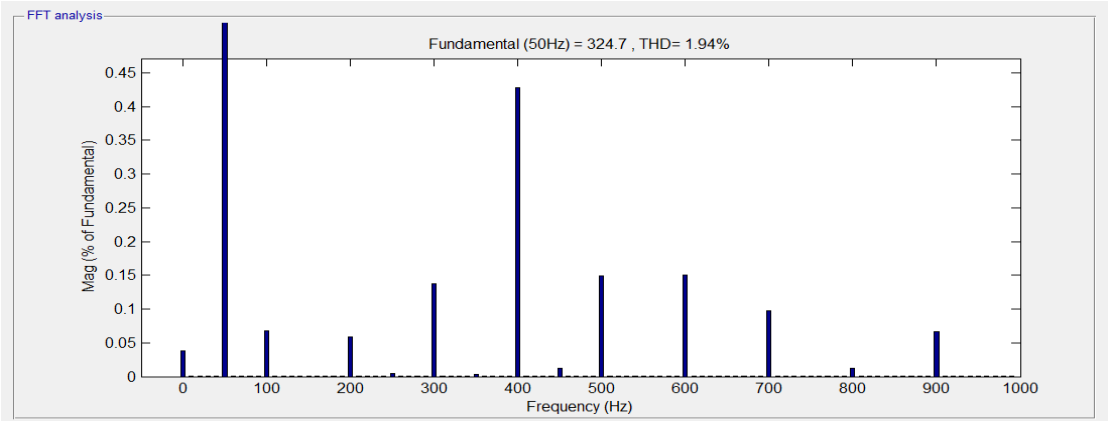


Fig. (13) spectrum of phase voltage (a) using FFT analysis.

on the other side, Fig. (14) illustrates the trajectory of the reference switching vector in $(\alpha, \beta, \gamma)$ plane. This trajectory is a circular shape; hence, it is the same as that in a 2-D traditional three-leg inverter.

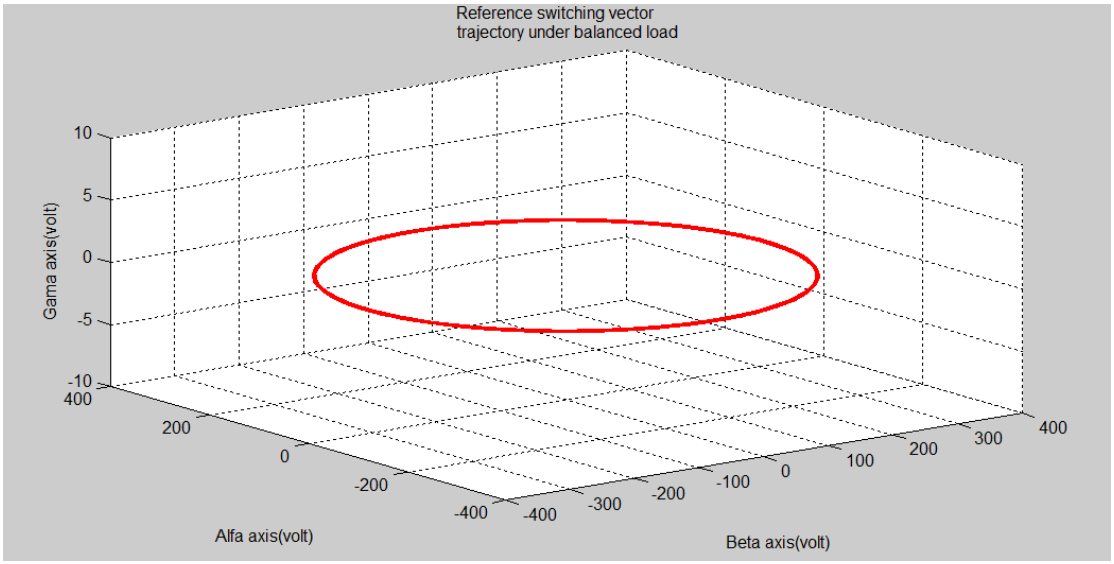


Fig. (14) a trajectory of the reference switching vector in $(\alpha, \beta, \gamma)$ plane.

Case 2: Unbalanced loading

In this case, a three-phase unbalanced load connected to inverter terminals ($R_a = 80\Omega$ , $R_b = 100\Omega, R_c = 150\ \Omega$). This leads to inject different magnitudes of phase currents in all phases with balanced angle displacement of 120° between these currents ($I_a = 4\angle 0^\circ$ , $I_b = 3.2\angle -120^\circ, I_c = 2.2\angle -240^\circ$ ). The waveforms of these currents and output voltages are shown in Fig. (15, 16) respectively. Fig. (17) illustrates the harmonic distribution spectrum of phase current (a).

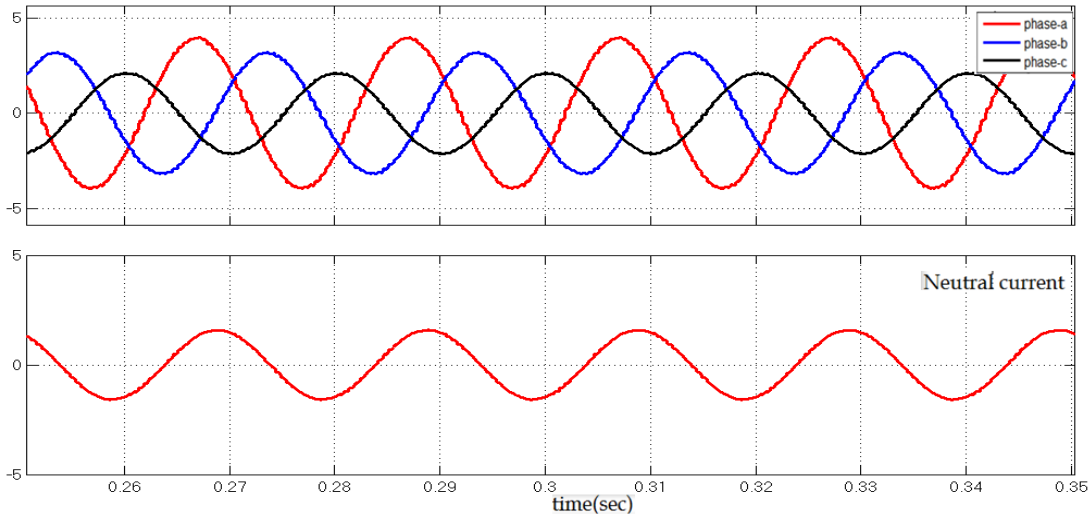


Fig. (15) the line and neutral current waveforms.

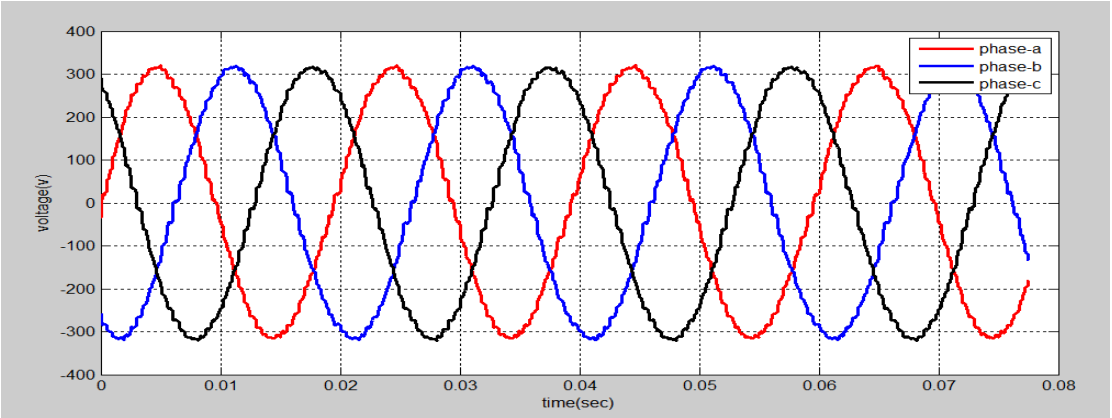


Fig. (16) output voltage waveforms.

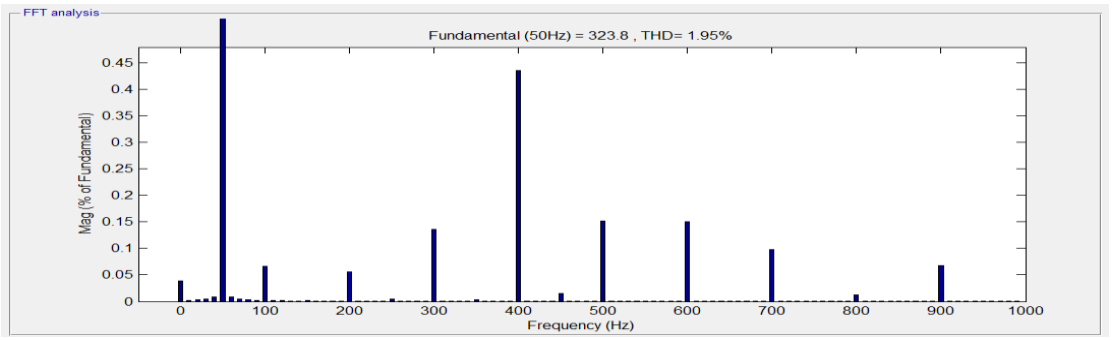


Fig. (17) output current spectrum of phase (a) using FFT analysis.

Fig. (18) illustrates the trajectory of the reference-switching vector in $(\alpha, \beta, \gamma)$ plane under unbalance load that appear as an elliptic shape, the shape change from circle shape in case-1 to ellipse shape as in case-2 due to the unbalanced loading.

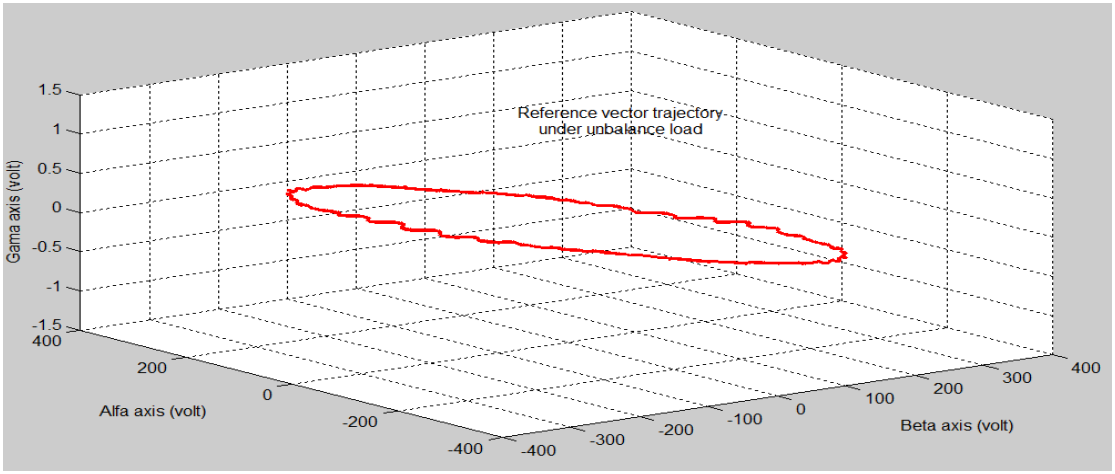


Fig. (18) a trajectory of the reference voltage vector in (α, β, γ) plane.

Case 3: Heavy unbalanced loading

In this case, assume phase (c) is in an open circuit condition and the other two phases are unbalanced. This will produce different currents in all phases are ($I_a = 2.12\angle 0^\circ$, $I_b = 4.0\angle -120^\circ$, $I_c = 0.0\angle -240^\circ$) A. The waveforms of these currents $I_a, I_b, I_c$ and $I_n$ shown in Fig. (19), the output voltages shown in Fig. (20), Fig.s (21) illustrate the harmonic distribution spectrum of the current in phase (a) and Fig.s (22) illustrate the trajectory of the reference switching vector in (α, β, γ) plane.

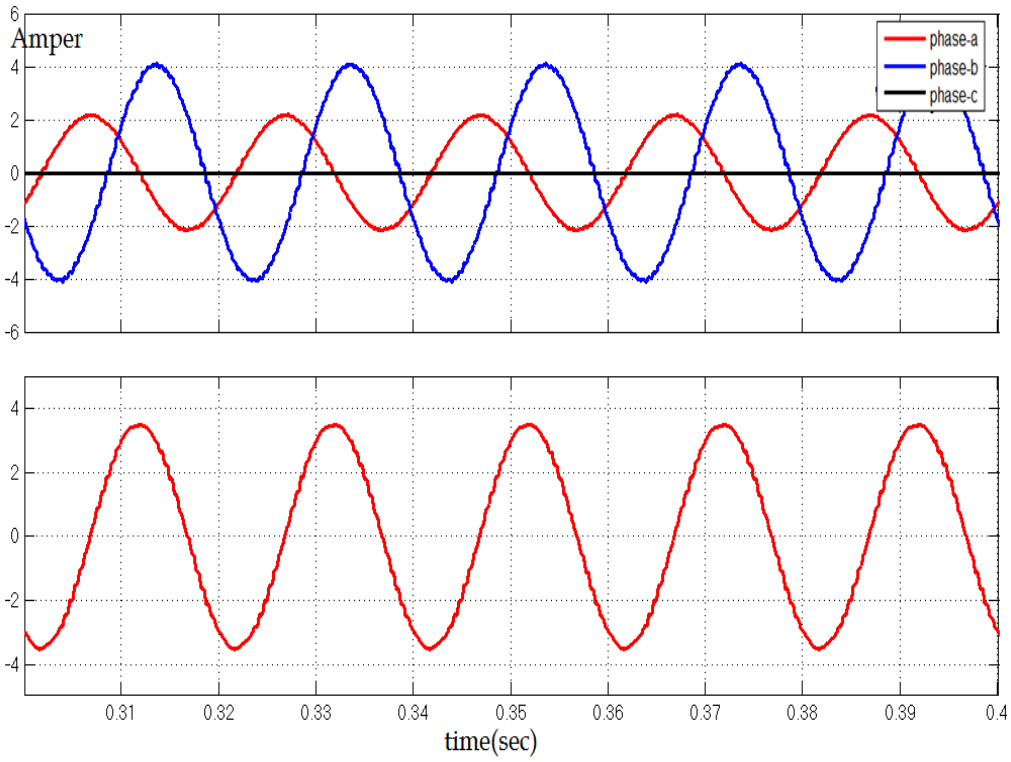


Fig. (19) the line and neutral current waveforms.

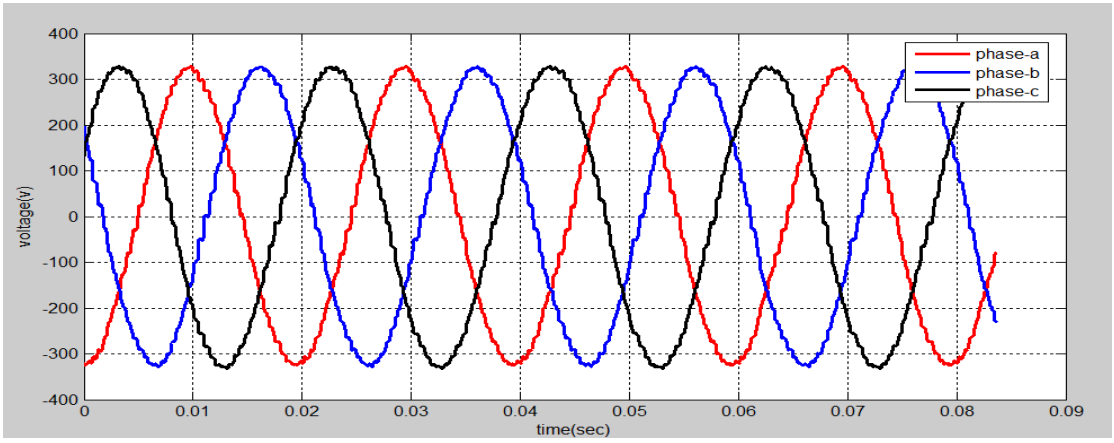


Fig. (20) output voltage waveforms.

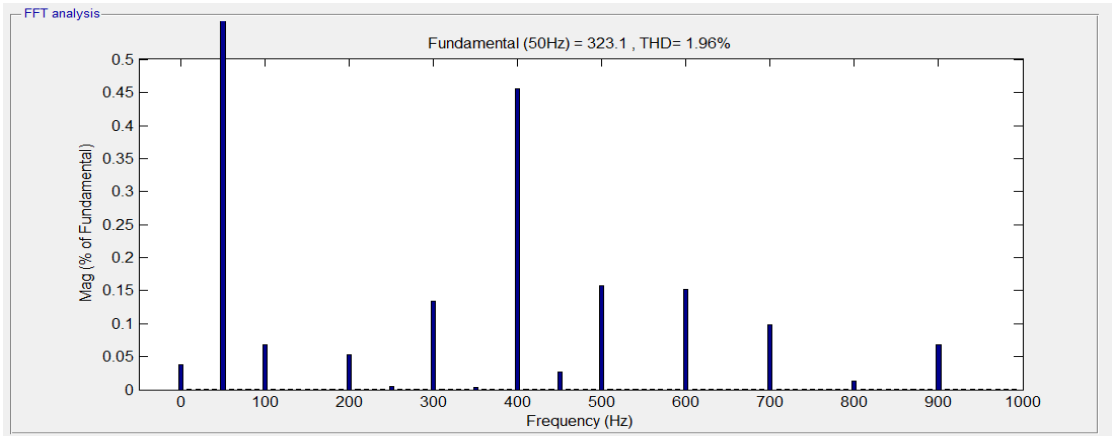


Fig. (21) output current spectrum of phase (a) using FFT analysis.

Fig. (22) illustrates the locus of the reference vector trajectory in $(\alpha, \beta, \gamma)$ plane under heavy unbalanced loading condition. As seen in this Fig. the shape became more elliptic as in the previous case, this proven that $(\gamma)$ axis are proportional with the magnitude of neutral current, which means that the angle $(\gamma)$ depend on neutral current.

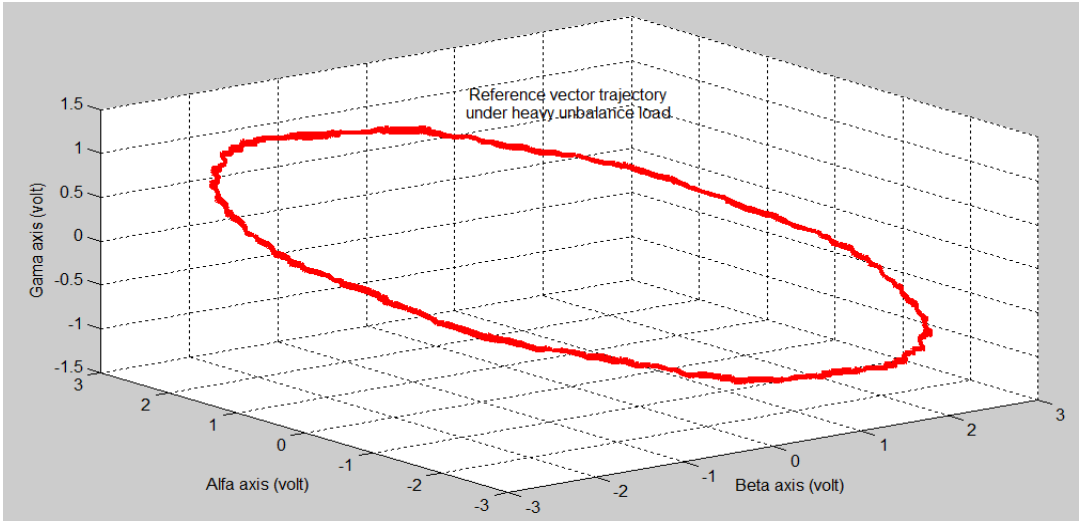


Fig. (22) a trajectory of the reference voltage vector in $(\alpha, \beta, \gamma)$ plane.

When the inverter fed an unbalanced load as mentioned in case-3 (the heavy unbalanced loading), the output voltage of the inverter when compared with a desired voltage for all phases are illustrated in Fig. (23). These Figures shows the capability of this model, performance to produce an output voltage same as reference command voltage.

on the other side, Fig. (24) show the pure sinusoidal waveform of the fundamental voltage in the same graph with the simulated four-legged switching network AC terminal output voltage for three phases respectively.

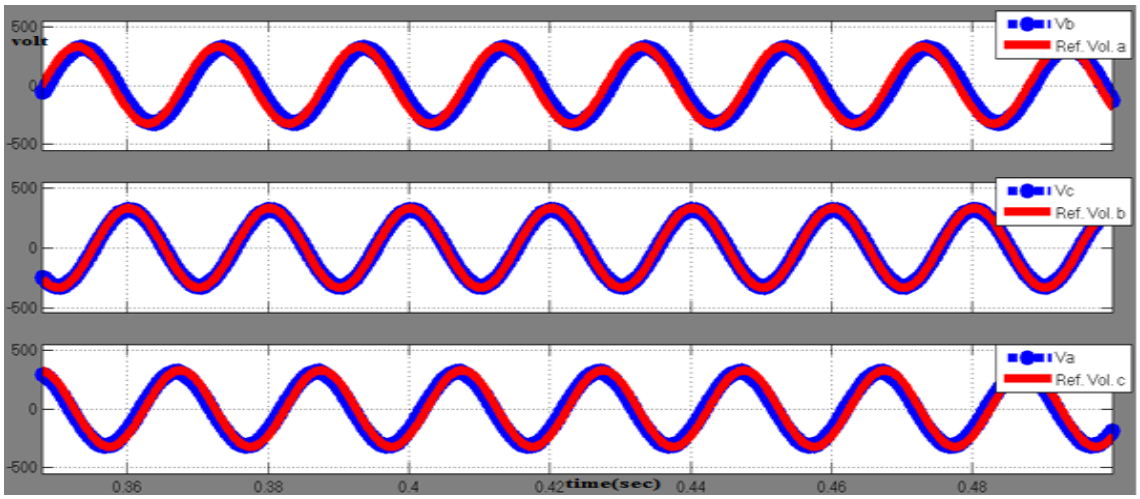


Fig. (23) Comparison between reference command voltages (red line) and inverter output voltages (blue line).

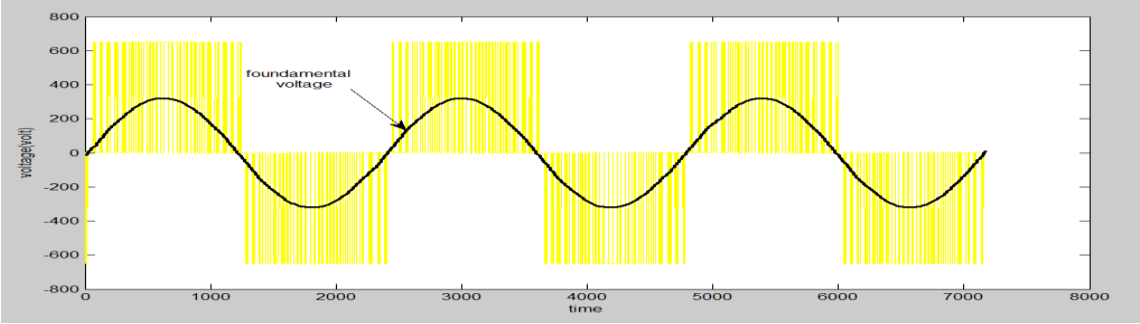


(a) Phase-a

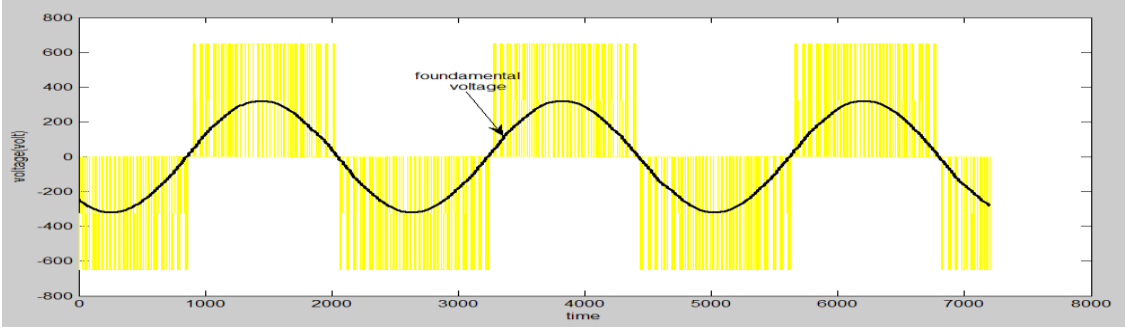


(b) Phase-b

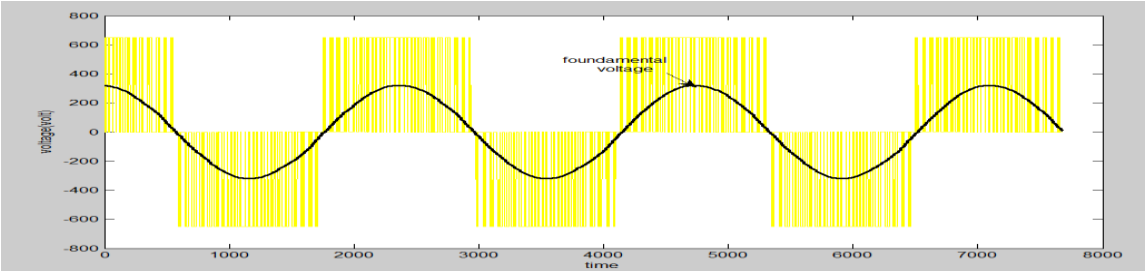


(c) Phase-c

Fig. (24) Inverter output phase voltages compared with the simulated four-legged switching network AC terminal output voltage.

## 8. Conclusions

This paper investigates the proposed three-phase four-leg SVPWM with a large signal inverter model in Matlab/Simulink.

Three different cases (balanced-unbalanced-heavy unbalanced) of the load operation condition are studied. Notice the increase in the load unbalance leads to increase of neutral current value and THD content in output voltages for the three cases consequently. The shape and the continuity of the reference vector trajectory presented in $(\alpha, \beta, \gamma)$ plane shows the performance change of 3P4L-VSI according to load type for different operation condition. The small difference between the desired reference voltage and the output voltage of the inverter for all phases approve the efficiency of this technique to handle the unbalanced load.

This result leads to the truth that the SVPWM solves the harmonic contents problem in spite of solving the unbalance in 3-phase load. This technique is compatible with hybrid power networks and it will be the most dominant in the future.

## 9. References

1. E. Rokrok and M. E. Hamedani, (2009). *"Comprehensive Control Scheme for an Inverter-Based Distributed Generation Unit"*. Iranian Journal of Science & Technology, Transaction B: Engineering, Vol. 33, No. B6, pp. 477-490.
2. Eyyup, D. Suleyman, C. and Ahmet, M. (2007). *"Output Voltage Control of A Four-Leg Inverter Based Three-Phase USP by Means of Stationary Frame Resonant Filter Banks"*. IEEE-IEMDC2007, Antalya-Turkey.
3. Mohammad, R. M. Mohd, F. R. Mohd, W. M. Ali, A. Gh. And Ali, R. R. (2016). *" An Improved Control Strategy for a Four-Leg Grid-Forming Power Converter under Unbalanced Load Conditions"*. Hindawi Publishing Corporation, Advances in Power Electronics, Volume 2016, Article ID 9123747,14 pages.
4. Pallagiri, V. and Chandra, R. (2015). *"Hybrid Renewable Energy Sources Based Four Leg Inverter for Power Quality Improvement"*. International Journal of Advanced Technology and Innovative Research, Vol. 07, Issue.06, p 1092-1098.
5. Min, Z. (2013). *" Investigation of Switching Schemes for Three-phase Four-Leg Voltage Source Inverters"*. Ph.D. Thesis, School of Electrical and Electronic Engineering, Newcastle University.

6. Richard, Z. Dushan, B. Prasad, V. Fred, C. L. (2002). *"Three-Dimensional Space Vector Modulation for Four-Leg Voltage-Source Converters"*. IEEE Trans. on Power Electronics, vol. 17, no. 3.
7. Riyadh, G. O. and Rabee, TH. (2014). " H. Thejel, *"Matlab/Simulink Modeling of Four-leg Voltage Source Inverter with Fundamental Inverter output Voltages Vector Observation"*. Iraq J. Electrical and Electronic Engineering, Vol.10, No.2.
8. Faleh, A. (2014). *"Dynamic Modeling and Analysis of the Three-Phase Voltage Source Inverter under Stand-Alone and Grid-Tied Modes"*. M.Sc. Thesis, Department of Electrical and Computer Engineering College of Engineering Kansas State University.
9. Riyadh, G. O. (2015). *" An Efficient SVPWM and Predictive Control of Four-leg Three-phase Voltage Source Inverter"*. PhD Thesis, Electrical Engineering Dept. College of Engineering, University of Basra.
10. Richard, Z. Dushan, B. Prasad, V. Hengchun, M. Fred, L. and Stephen, D. (1997). *"A Three-phase Inverter with A Neutral Leg with Space Vector Modulation"*. IEEE, The Twelfth Annual Conf. and Exp. on Applied Power Electronics, APEC '97 Conf. Proc. pp. 857 - 863 vol.2.
11. Richard, Z. Dushan, B. Prasad, V. (1997). *"Analysis and Comparison of Space Vector Modulation Schemes for a Four-Leg Voltage Source Inverter"*. IEEE, Applied Power Electronics Conf. and Exp., APEC '97 Conf. Proc., pp. 864 – 871, Vol. 2.
12. Dhaval, C. P. Rajendra, R. S. and Mukul, C. C.(2010). *"Three-Dimensional Flux Vector Modulation of Four-Leg Sine-Wave Output Inverters"*. IEEE Transactions on Industrial Electronics, Vol. 57, No.4.
13. Ayhan, O. and Zekiye, E.(2014). *"Optimal Digital Control of a Three-Phase Four-Leg Voltage Source Inverter"*. Turkish Journal of Electrical Engineering and Computer Science, Vol. 201.